Chapter

Probing Solvation Effects in Binary Solvent Mixtures with the Use of Solvatochromic Dyes

Ioanna Deligkiozi and Raffaello Papadakis

Abstract

In this work three molecules exhibiting dual sensing solvatochromic behaviors are examined in the context of solvation in binary solvent mixtures (BSMs). The compounds studied involve two functional groups with high responsiveness to solvent polarity namely pentacyanoferrate(II) (PC) and azo groups. Two of these compounds are [2]rotaxanes involving *alpha-* or *beta-* cyclodextrin (CyD) and the third is their CyD-free precursor. The dual solvatochromic behavior of these compounds is investigated in water/ethlylene glycol (EG) mixtures and their dual solvatochromic responses are assessed in terms of the intensity of solvatochromism and the extent of preferential solvation. To achieve this the linear solvation model by Kamlet, Abboud and Taft [*J. Organomet. Chem.* 1983, *48*, 2877–2887] and the two-phase model of solvation by Bagchi and coworkers [*J. Phys. Chem.* 1991, *95*, 3311–3314] are employed. The influence of the presence or lack of CyD (*alpha-* or *beta-*) on these dual solvatochromic sensors is analyzed.

Keywords: solvatochromic dyes, rotaxanes, preferential solvation, (non) specific solute-solvent effects, azo dyes

1. Introduction

Nowadays, solvatochromic probes (SPs) are regularly utilized in various types of applications which require sensing of environmental/medium effects in either a qualitative or a quantitative manner [1–9]. Today there is a large variety of published solvatochromic dyes corresponding to different media, e.g. organic solvents [8, 10], ionic liquids [10, 11], solvent mixtures [10, 12–15] or solvent comprising polarity modifiers [16]. What often appears to be challenging is the choice of a suitable solvatochromic probe for the description of a physicochemical problem encompassing solvent polarity effects. It has been observed that for the same solvent/cosolvent mixture, different solvatochromic dyes may provide different quantitative results [17, 18]. Indeed in many cases, different spectroscopic techniques applied on the same ternary system solvent/cosolvent/probe(solute) may provide different results. Therefore, probing solvent polarity effects and preferential solvation (PS) phenomena occurring in solvent mixtures of two or more

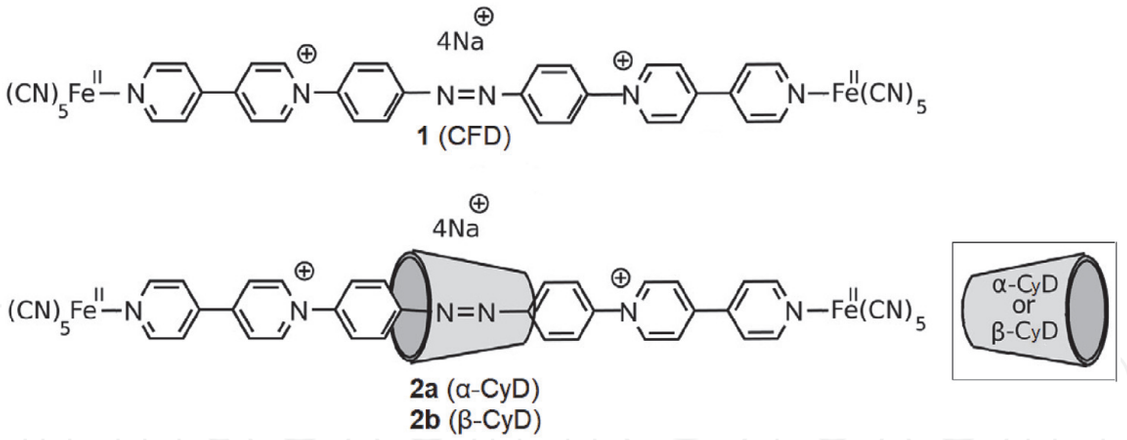

Figure 1.
The three solvatochromic compounds involved in this study.

solvents are considered as highly difficult tasks [17]. The complexity of those physicochemical problems is high and the interpretation of the solvent-solvent or solute-solvent effects sensed by SPs needs to be carefully undertaken. In this work, the authors examine the solvatochromic responses of two probing groups: the azo-group and the pentacyanoferrate(II) group of three molecules dissolved in binary solvent mixtures (BSMs) involving water and ethylene glycol (EG). From the three molecules employed two are [2]rotaxanes involving *alpha-* or *beta-* cyclodextrin (CyD) (compounds **2a** and **2b** respectively, **Figure 1**) and the third is their precursor lacking a CyD wheel (compound **1**, **Figure 1**; in the text will be called cyclodextrin-free dumbbell-like compound or CFD). All three are recently developed solvatochromic compounds [19] and they involve the same π-conjugated viologen-based linear skeletons bearing an azobenzene bridge and pentacyanoferrate(II) end-groups (**Figure 1**). The aforementioned compounds fall under the umbrella of an important family of multifunctional dyes primarily because of the high technological and industrial importance of azobenzene dyes [20–22] as well as the pronounced chromic and redox behavior [23], photochromism [24], photoconductivity [25] and strong electron withdrawing aptitude of viologens (also known as paraquats) [23, 26]. This strong electron accepting capacity of para- and monoquats is vital for the development of push-pull systems [27–30]. Towards the latter milestone the use of suitable electron donating substituents is vital. Papadakis et al. has shown that pentacyanoferrate(II) units can trigger an intense solvatochromic behavior in such systems in various types of media [14, 16, 30, 31] and more recently Deligkiozi et al. hinted that the $n \rightarrow \pi^*$ transitions of the azo group in **1** and **2a,b** are sensitive to solvent polarity [19]. In this work the dual solvatochromic sensing of these compounds is thoroughly examined in terms of solvent-solute, solvent-solvent and preferential solvation effects. In this work water/ethylene glycol mixtures were chosen as perfect BSM candidate-models of dipolar media with substantial contributions in the development of specific effects (mainly H-bonding).

2. Materials and methods

2.1 General information

All correlations (single or multi- parameter linear, polynomial regressions and contribution analyses were carried out using statistical software *R* (ver.:3.5.3). Integrations as well as the graphical determination of isosolvation points were all performed using QtiPlot (ver.: 0.9.9).

All compounds involved in this work (**1** and **2a,b**; **Figure 1**) have been reported in earlier publication by the author and coworkers and their synthesis, isolation and spectral analysis have been also thoroughly described [19]. All solvatochromic UV–Vis shifts have been recorded on a Perkin-Elmer Lambda 25 UV/Vis spectrophotometer. The deconvolutions of all UV–Vis spectra were implemented according to previous work [19].

2.2 Examining the stability of compounds 1,2a,b in solution

All solvatochromic compounds used in this work are isolated as stable solid compounds of green-blue color. The measurements presented were conducted in fresh solutions of each compound in the desired H_2O/EG mixtures (typically prepared 15 min prior to measurement). That time corresponds to the equilibration time (each sample was vigorously stirred after mixing). Directly after this period of time their electronic absorption spectra were recorded. It was observed that in all cases the solutions remained unmodified as concluded through check of the absorbances of the bands maxima which were found to be stable for at least 30 minutes after equilibration. This observation clearly indicates that all three compounds are stable in solution and therefore suitable for the current investigation.

2.3 Preferential solvation model

In this work a renowned PS model is employed in order to describe PS phenomena occurring in BSMs comprising solvatochromic solutes. The model was introduced by Bagchi and coworkers about thirty years ago and is also known as "the two-phase model of solvation" (TPMS) [32–34]. TPMS considers that solvent molecules in a BSM are distributed between a local phase and a bulk phase according to Eq. 1. The local phase lies in the vicinity of the solvation area.

$$\overline{S_2} + S_1 \rightleftharpoons \overline{S_1} + S_2 \tag{1}$$

In Eq. 1 S_1 and S_2 symbolize the two mixed solvents in the bulk phase while $\overline{S_1}$ and $\overline{S_2}$ symbolize the two solvents in the solvation (local) phase. Throughout this work water will be considered as S_1 whereas EG as S_2. At the equilibrium described by Eq. 1, PS constant (K_{ps}) will be related to an expression comprising both solvent-solvent solute-solvent interaction energies (Eq. 2).

$$kTlnK_{PS} = [\epsilon_{S2} - \epsilon_{S1}] + \left[(N_1 - N_2)\epsilon_{12} - \left(N_1^0 - N_2^0\right)\epsilon_{12}^0 - N_1\epsilon_{11} + N_1^0\epsilon_{11}^0 + \right.$$
$$\left. + N_2\epsilon_{22} - N_2^0\epsilon_{22}^0 + \frac{(\epsilon_{11} - \epsilon_{22})}{2} - \frac{\left(\epsilon_{11}^0 - \epsilon_{22}^0\right)}{2} \right] \tag{2}$$

In Eq. 2 ϵ_{Si} are the interaction energies among the solute and i-solvent while ϵ_{ij} corresponds to the interaction energies between solvents i and j. N_i corresponds to the number of i-solvent molecules. The bulk phase in solvent molecule numbers is designated with the superscript 0. It is noteworthy that Eq. 2 involves two terms. The first bracketed term in the right-hand side of the equation corresponds to the contribution of solute-solvent interactions, while the terms in the second bracket describe the solvent non-ideality effects.

Finally, Eq. 3, provides K_{ps} (the preferential solvation constant) related to both bulk (x) and local (y) solvent mole fractions along with the measured transition

energies of the indicator solute (E_T) observed in neat solvent S_1 ($E_{T,1}$), neat solvent S_2 ($E_{T,2)}$ and the mixture of S_1 and S_2 ($E_{T,\mathrm{m}}$).

$$K_{PS} = \frac{y_1 x_2}{y_2 x_1} = \frac{E_{T,m} - E_{T,2}}{E_{T,1} - E_{T,2}} \bullet \frac{x_2}{x_1} \tag{3}$$

2.4 Applying the CNIBS/R-K equation

In order to determine isosolvation points (see below) pertaining to PS occurring in solutions of **1** and **2a,b** in aqueous EG, Redlich–Kister (CNIBS/R–K) equation [35], was employed so as to algebraically describe the dependence of experimental transition energy E_T ($n \rightarrow \pi^*(azo)$ and Metal to Ligand Charge Transfer (MLCT)) on solvent/cosolvent bulk mole fractions (x_1, x_2) (Eq. (4)). In this work water is considered as solvent S_1 (i.e. water mole fraction is x_1). Noteworthy, Eq. 4 yields E_T values corresponding to neat solvents S_1 and S_2 ($E^0_{T,1}$ *and* $E^0_{T,2}$) when any of x_2 and x_1 is set to 0 respectively.

$$E_{T,m} = x_1 E^0_{T,1} + x_2 E^0_{T,2} + x_1 x_2 \sum_{j=0}^{k} A_j (x_1 - x_2)^j \tag{4}$$

2.5 Determining isosolvation points

For a BSM involving solvents S_1 and S_2 and a solvatochromic solute, when $x^T_{iso}(S_2) < 0.5$ then PS of the solute by solvent S_2 is observed and vice versa when $x^T_{iso}(S_1) > 0.5$ [18] (where T corresponds to the transition of interest i.e. MLCT (PCF) or $n \rightarrow \pi^*(azo)$ for this study).

$$x^T_{iso} = x^T \text{ at which } E_{T,m} = \frac{E^0_{T,1} + E^0_{T,2}}{2.}$$

For the determination of x^T_{iso} the polynomial expressions obtained through Eq. 5 were utilized. $E_{T,m} = f(x_1)$ were first plotted and then x^T_{iso} were determined graphically using the data reader tool of Qtiplot 0.9.9.

2.6 Quantifying the difference in the extent of PS

In order to quantify the difference of the extent of PS in aqueous EG through the two different types of transitions (MLCT(PCF) or $n \rightarrow \pi^*(azo)$) of **1,2a,b** the following integrals difference ($\boldsymbol{\Delta} \int$) was employed.

$$\boldsymbol{\Delta} \int = \left(\int_0^1 y^{n \rightarrow \pi^*}_{EG}(x_{EG})\, dx_{EG} \right) - \left(\int_0^1 y^{mlct}_{EG}(x_{EG})\, dx_{EG} \right) \tag{5}$$

In Eq. 5$y^{n \rightarrow \pi^*}_{EG}$ and y^{MLCT}_{EG} are the local EG molar fractions determined through the TPMS methodology peraining to the $n \rightarrow \pi^*(azo)$ and MLCT (PCF) transitions respectively.

2.7 Single parameter regression analyses

To understand the role of various solvatochromic parameters expressing solvent polarity, single regression analyses were implemented (general Eq. (6)). SSP-LSERs

$$E_{T,m} = E^0_{T,m} + p_i \cdot SP_i, r^2 \quad (6)$$

Where $T = MLCT\ or\ n \rightarrow \pi^*$ and SP a solvent polarity parameter (in this work: E^N_T, π^*, α, or β). r^2: correlation coefficient.

2.8 KAT equation and contribution analysis

Moreover a multiparametric model was employed in order to assess the relative contribution of various solvatochromic parameters expressing solvent polarity, simultaneously. That model is the LSER introduced by Kamlet Abboud and Taft (KAT equation). This renowned LSER (Eq. 7) can provide information on the importance of dipolarity/polarizability, Hydrogen bond donor (HBD) acidity and Hydrogen bond acceptor (HBA) basicity of neat solvents or solvent mixtures.

$$E_{T,m} = E^0_{T,m} + s\pi^* + a\alpha + b\beta \quad (7)$$

Where

$$T = MLCT\ or\ n \rightarrow \pi^*$$

Through Eqs. 8–9 it is possible to determine the relative contribution (r_{s_i}) of each of the involved parameters. The procedure has thoroughly been described in previous works [28, 31, 36].

$$r_{s_i} = \frac{\sigma'_i}{\sum_{i=1}^{n} \sigma'_i} \quad (8)$$

and

	$E_{n\rightarrow\pi^*}$ $(kcal.mol^{-1})$[a]			E_{MLCT} $(kcal.mol^{-1})$[a]		
x_{EG}	**1**	**2a**	**2b**	**1**	**2a**	**2b**
0	73.12	74.26	74.26	51.46	49.02	50.71
0.051	71.48	73.88	73.50	49.06	48.67	48.85
0.097	72.38	73.50	73.88	48.44	47.16	47.18
0.139	70.77	72.38	72.57	47.26	46.15	47.18
0.178	69.91	71.48	71.48	46.23	45.36	46.67
0.212	69.73	71.48	71.48	46.34	44.50	46.50
0.245	69.73	71.48	71.84	45.29	44.10	46.50
0.392	69.73	70.95	71.66	45.78	43.74	44.85
0.492	69.73	70.77	71.12	45.06	42.94	43.66
0.659	69.73	70.77	70.77	43.95	41.85	42.83
0.854	69.73	70.77	70.77	42.94	41.08	41.94
1	69.73	70.42	70.42	41.60	40.35	40.94

[a]*Data from reference: [19].*

Table 1.
Solvatochromic shifts of ***1*** *and* ***2a,b*** *in aqueous EG and solvent polarity parameters.*

$$\sigma_i' = |\sigma_i| \sqrt{\frac{\sum_{j=1}^{m} \left(S_{ij} - \overline{S_i}\right)^2}{\sum_{j=1}^{m} \left(E_{Tj} - \overline{E_T}\right)^2}} \tag{9}$$

where S_i corresponds to the correlation to each of any of the three parameter involved in Eq. 8 for the various solvent/cosolvent molar ratios examined (number of different mole ratios examined in this work: m = 12; see **Table 1**).

3. Results and discussion

3.1 The bisensing solvatochromic compounds 1 and 2a,b

Recently Deligkiozi et al. [19] and subsequently Papadakis et al. [37] reported on the solvatochromic behavior of compounds **1**, **2a-b** (**Figure 1**). It has been pointed out that the energy of the MLCT transition in these compounds is intensely dependent on the polarity of the environment and its nature and characteristics have been thoroughly described in a series of research works [14–16, 19, 30, 31]. These compounds have been studied in a rather narrow solvent polarity range and specifically in aqueous EG mixtures as well as in neat water and EG. All three compounds are very soluble in both those solvents and their mixtures. Despite the small solvent polarity difference observed when moving form water to EG, the recorded difference in MLCT energy of **1** and **2a,b** was reported to be significantly high, following the sequence:

$$\left|\Delta^{EG}_{H_2O}(\tilde{\nu}_{MLCT}\mathbf{1})\right| = 3451\ cm^{-1} > \left|\Delta^{EG}_{H_2O}(\tilde{\nu}_{MLCT}\mathbf{2}\boldsymbol{a})\right| = 3419\ cm^{-1} >$$

$$> \left|\Delta^{EG}_{H_2O}(\tilde{\nu}_{MLCT}\mathbf{2}\boldsymbol{b})\right| = 3033\ cm^{-1}.$$

Interestingly, all three compounds also exhibit another transition which is significantly influenced by solvent polarity. The latter is attributed to the azobenzene group and corresponds to the forbidden $n \rightarrow \pi^*$ transition of the lone pairs of electrons of the azo nitrogen atoms and is located at λ ranging within 385–410 nm strongly depending on the polarity of the solvent. The solvatochromism of azobenzene-based compounds has been thoroughly investigated in the past and there is clear evidence of the solvent dependent nature of the $n \rightarrow \pi^*$ and $\pi \rightarrow \pi^*$ azo transitions [38–41]. This comes as no surprise as the nitrogen atoms of the azo group can readily interact with solvent molecules (in case of compound **1**) or the interior groups of CyDs (*alpha-* for **2a** and *beta-* for **2b**). Typically, the energy of the $n \rightarrow \pi^*$ transition shifts about 6 nm hypsochromically just upon insertion of the CyD wheel. For instance while in neat water $\lambda_{(n \rightarrow \pi^*)} \cong$ 391 nm for the CFD compound (**1**) while $\lambda_{(n \rightarrow \pi^*)} \cong$ 385 nm when the CyD wheel is threaded and stationed around the azobenzene group (same value for both **2a** and **2b**). Comparable shifts are observed at various mole fractions of water in aqueous EG (see **Table 1**). Yet, the effect of solvents is much more important as shifts of even 25 nm are observed when simply moving from water to EG i.e. two solvents with many similarities when it comes to solvent polarity and structuredness [18]. The observed shifts recorded followed the trend:

$$\left|\Delta^{EG}_{H_2O}(\tilde{\nu}_{n \rightarrow \pi^*}\mathbf{1})\right| = 1186\ cm^{-1} < \left|\Delta^{EG}_{H_2O}(\tilde{\nu}_{n \rightarrow \pi^*}\mathbf{2}\boldsymbol{a})\right| = \left|\Delta^{EG}_{H_2O}(\tilde{\nu}_{n \rightarrow \pi^*}\mathbf{2}\boldsymbol{b})\right| = 1345\ cm^{-1}.$$

It is important to note here that the $n \rightarrow \pi^*$ transition is convoluted with the MLCT and $\pi \rightarrow \pi^*$ transitions and a thorough deconvolution analysis has been already published recently [19]. In this work the used values of the energies for $n \rightarrow \pi^*$ and MLCT transitions for **1** and **2a,b** correspond to the aforementioned published deconvolution values (see **Figure 2** and **Table 1**).

Taken together, there is clear evidence that all three compounds are considered to be bisensing as they involve two functional groups (FC and azo groups) both responding to solvent polarity changes however at different extents (**Table 1**) as it will be thoroughly analyzed.

3.2 Resonance structures of compounds 1 and 2a,b

For a better understanding of the dual solvatochromic behavior of all compounds the analysis of their resonance structures is vital. While resonance structure **I** (**Figure 3**) is more important in the electronic ground state and comprises Fe(II) and the all-aromatic structure of the ligand (L), Resonance structure **II** (**Figure 3**) becomes more important in the MLCT excited state of molecules **1** and **2a,b**. The latter resonance structure comprises the oxidized metal center (Fe(III)) and the quinoidal structured ligand as a result of the acceptance of an electron transferred by Fe(II) upon oxidation occurring via absorption of light (MLCT). (Structure **II** is one of the corresponding resonance structures of the type: $[(\mathbf{Fe^{III}} - \mathbf{L^{+\bullet}})]$.

Finally, structure **III** (**Figure 3**) retains the oxidized Fe^{III} center however displays the possibility of stabilization of the $>N^{+\bullet}$ by the azo group. (It is noteworthy that the azo group is known to stabilize carbocations in a similar fashion [42]). The interplay between Resonance structures **II** and **III** can be alternatively written as: $[(\mathbf{Fe^{III}}-(\boldsymbol{py}^{+\bullet}) - \boldsymbol{azo}] \leftrightarrow [(\mathbf{Fe^{III}}-(\boldsymbol{py}^{+}) - \boldsymbol{azo}^{\bullet}]$.

The latter interaction of the azo group with its partly reduced neighboring viologen pyridin heterocycle obviously influences the $n \rightarrow \pi^*$ transition of the azo group which is in turn largely influenced by its interactions in solution with solvent molecules (this applies only to the case of compound **1**) or the interactions with the CyD interior environment (this is obviously valid only for rotaxanes **2a** and **b**). In any case, through Structures **II** and **III** it becomes obvious that the $n \rightarrow \pi^*$ transitions and the solvatochromism of the azo group is largely influenced by the $(Fe^{II} - L)$ system attached to it in π-conjugation.

Frontier orbital representations of the tetraanion of dye **1** ($\mathbf{1}^{4-}$) (for more details see ref.: [19]) also support the fact that the FC groups and azo groups are behaving as electron donating since the HOMO are mostly localized in the regions of the FC and azobenzene moieties (**Figure 4**). On the other hand, LUMO are mostly localized around the quaternized electron deficient viologen parts of the solvatochromic compounds (**Figure 4**). This is an additional hint to the dominating resonance structures presented in **Figure 3**.

3.3 Solute-solvent interactions

It is also noteworthy that in cases **2a,b** the $n \rightarrow \pi^*$ transition of the azo group is even more affected by the behavior of the 4,4′-bipyridine-Fe(II) system (which is in π-conjugation with the azobenzene moiety) than happens in case **1**. This is associated with the fact that CyD (either *alpha*- or *beta*-) does not allow any direct interaction of the azo group with any of the solvents (water or EG; see **Figure 5**).

It is known that solvents with $logP_{oc/w} < -0.3$ cannot penetrate the highly lipophilic cavity of cyclodextrins (for EG it is $logP_{oc/w} = -1.3 < -0.3$ rendering it very hydrophilic to enter the CyD cavity ($P_{oc/w}$ is the 1-octanol/water partition coefficient) [43]. This is clearly manifested by the linear correlation between the

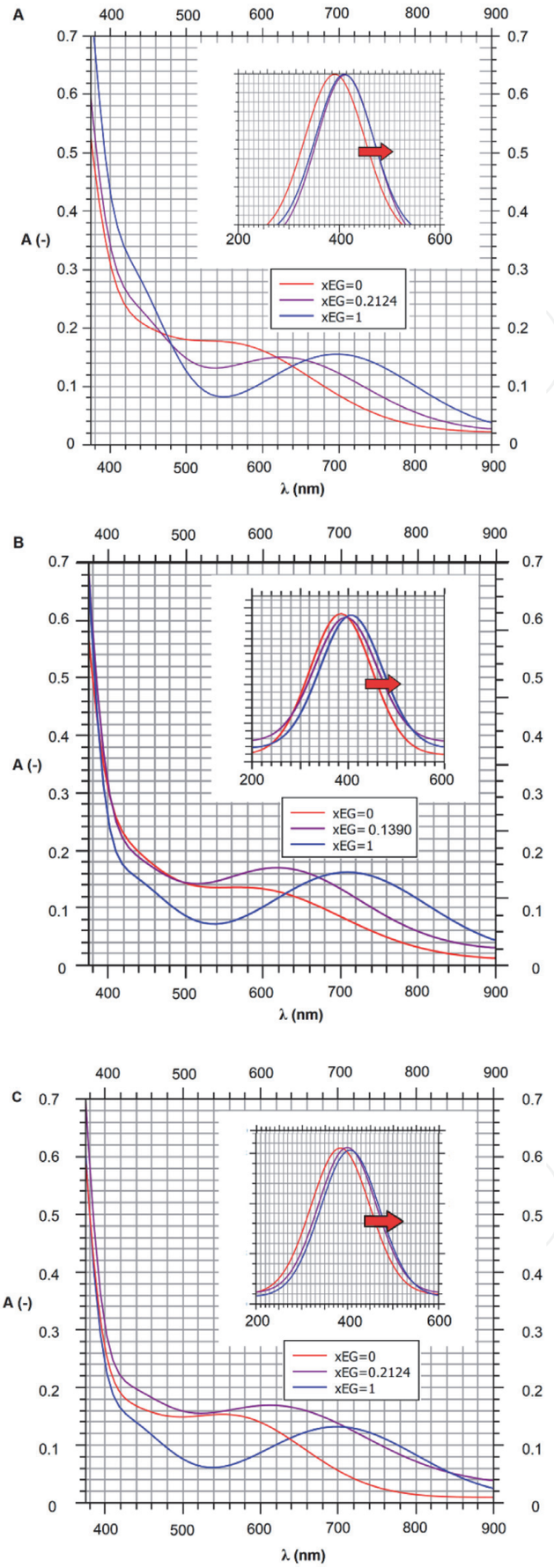

Figure 2.
The electronic spectra of compounds A) **1**, *B)* **2a**, *and C)* **2b** *recorded in water, EG and selected water/EG mixtures. Displayed wavelength range 380–900 nm. Insets indicate the* n→π* *bands after deconvolution.*

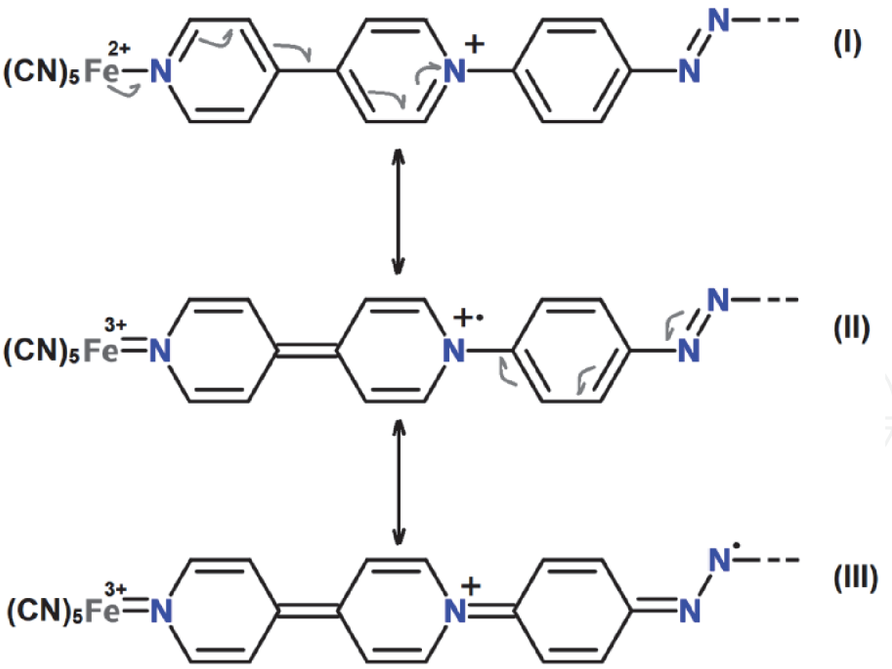

Figure 3.
Characteristic resonance structures of compound 1.

MLCT and $n \rightarrow \pi^*$ transitions energies of **2a,b** at various mole fractions of EG (see **Figure 6**). In case of compound **1** such a linear behavior is not observed (**Figure 6**).

3.4 Quantification of the solvatochromism of the FC and azo groups

A pertinent way to quantify, predict and rationalize solvent effects is the use of linear solvation energy relationships (LSERs). This approach has been employed in numerous research works focusing on solvent effect on a large variety of physicochemical properties [8, 10, 44–46]. The solvatochromism of PC complexes has been thoroughly investigated in this fashion as well [15, 16, 19, 31]. Particularly in case of PC complexes bearing pyridinic ligands (such as **1** and **2a,b**) it has been shown that the MLCT transition energies are largely affected by the dipolarity/polarizability of the medium as well as hydrogen bond donor (HBD) and Lewis acidity [15, 16, 19, 31]. Deligkiozi et al. recently reported the corresponding correlations and furthermore hinted that the energy of the $n \rightarrow \pi^*$ of the azo group in **1** and **2a,b** is also sensitive to solvent polarity changes, thus revealing a dual sensing aptitude of solvent polarity for these compounds [19]. Nevertheless, that work mainly focused on the MLCT transitions of these three compounds. Herein, the author focuses further on the solvents effects on the solvatochromic behavior of the azo group of **1** and **2a,b** and examines this dual solvatochromic behavior.

Plots $E_{n\rightarrow\pi^*}$ *vs* E_{MLCT} (**Figure 6**) indicate fairly good linear correlations for the two rotaxanes (**2a,b**) however a severe deviation from linearity in case of the CFD compound (**1**). This is a stimulating finding pertaining to the structural diversity between the two rotaxanes and their CFD precursor. What this finding implies is that for compounds **2a,b** the medium responsive behavior of the azo group (expressed through $n \rightarrow \pi^*$ transitions) is expected to be analogous to that of the FC groups, at least qualitatively. Furthermore, the duality of solvent polarity sensing aptitude of **1** is anticipated as more pronounced. In order to shed light on these two hypotheses a series of correlations utilizing monoparametric LSERs was accomplished for all three compounds.

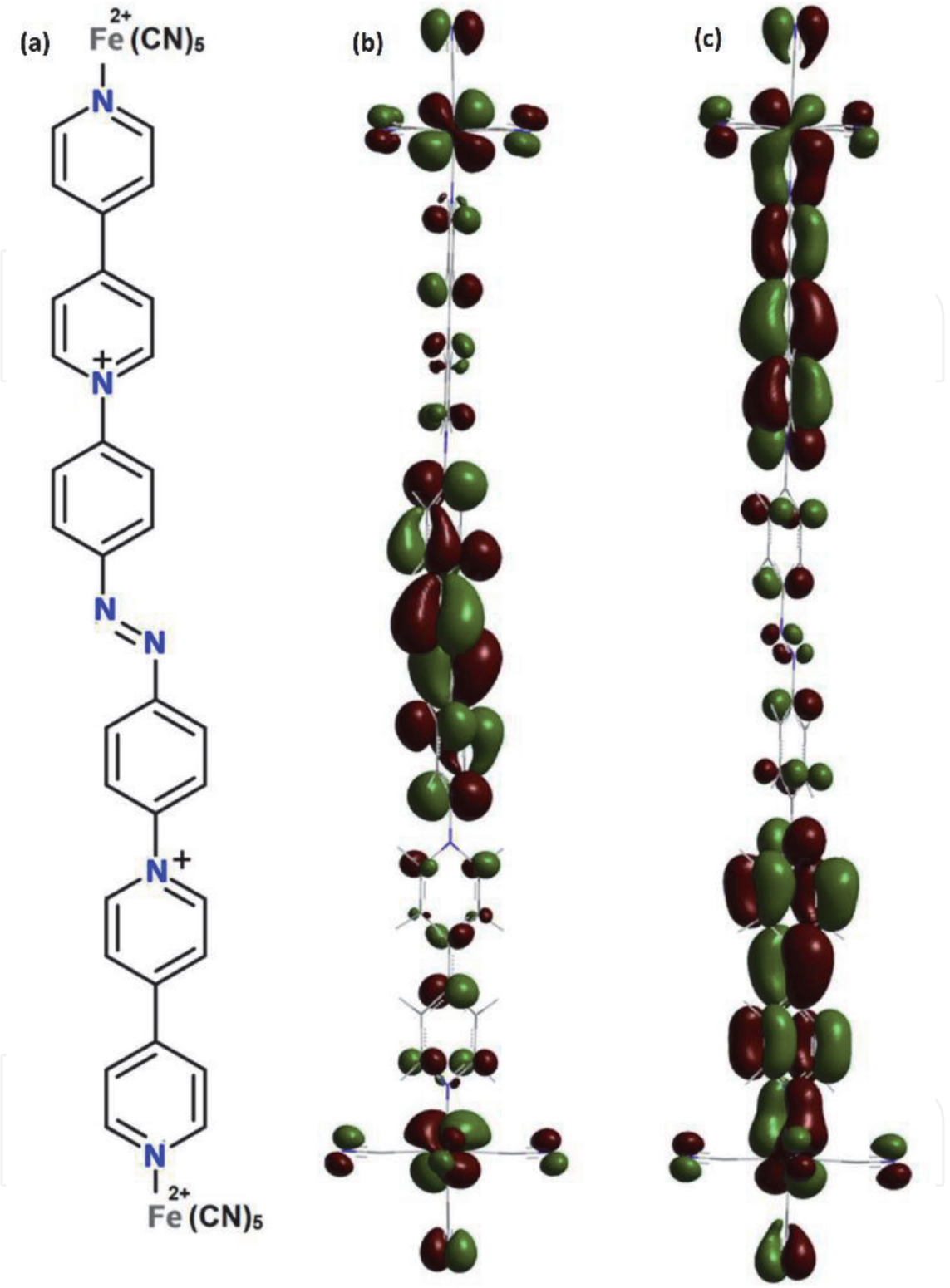

Figure 4.
Structure of the anion of dye **1** *(a) and illustrations of the frontier molecular orbitals (MOs) of the anion of the anion if dye* $\mathbf{1}^{4-}$*: HOMO (b) and LUMO (c) calculated on the B3P86/6–311++G(d,p) basis/vacuum (0.02 contour plots).*

3.5 Single solvent polarity parameter involving LSERs

Single solvent polarity parameter involving LSERs (SSP-LSERs) were employed in order to investigate the importance of various solvent polarity parameters on $n \rightarrow \pi^*$ and MLCT transitions of **1** and **2a,b**. The SPPs utilized were the following:

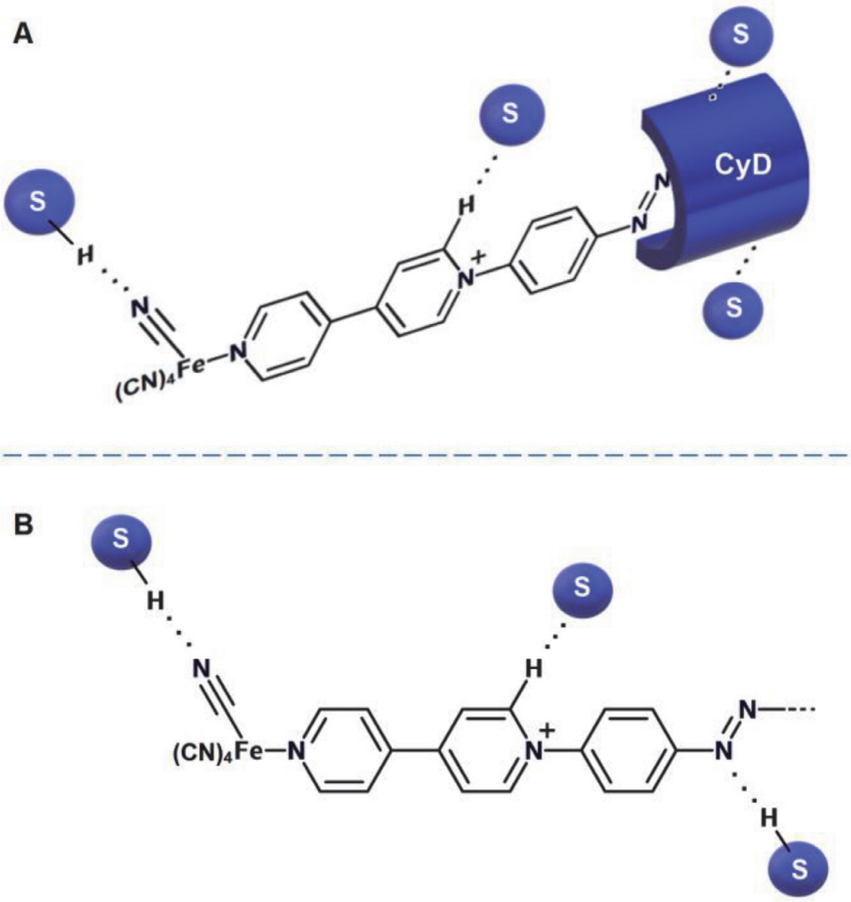

Figure 5.
*Illustration of the possible solute-solvent interactions in A) the rotaxanes **2a,b** and B) their CFD precursor **1** (S represents a solvent molecule or a solvent-cosolvent complex).*

Reichardt's solvent polarity scale: E_T^N, π^*, α, and β. The latter three are parameters involved in KAT equation expressing dipolarity/polarizability, HBD-acidity, and HBA-basicity respectively [47]. It is obvious that rotaxanes **2a** and **2b** exhibit $n \rightarrow \pi^*$ transition energies which correlate linearly with Reichardt's polarity scale E_T^N varying within 1.000 for water and 0.790 for EG (**Figure 7**). In contrast, the fitted curve between $n \rightarrow \pi^*$ transition energies of **1** and E_T^N is not a straight line (**Figure 7**). This finding for the solvatochromism of the azo group of compound **1** implies a different behavior compared to either of the rotaxanes **2a,b** or even the MLCT transitions of the same compound. Moreover, as E_T^N is a measure of dipolarity and Lewis acidity of the medium, the aforementioned results indicate a significantly lower dependence of the $n \rightarrow \pi^*$ energies on these solvent polarity features for compound **1**. Similar results were obtained for the correlations between $n \rightarrow \pi^*$ transitions for all three compounds and parameters π* and α, expressing solvent dipolarity/polarizability and HBD-acidity respectively (**Figures 7** and **8**). In those cases compound **1** continued to differ from compounds **2a-b.** This comes as no surprise as the connection between E_T^N scale and KAT parameters π* and α is known (as already mentioned E_T^N is a measure of solvent dipolarity and Lewis acidity) [10]. Very interestingly, the $n \rightarrow \pi^*$ energies of compound **1** correlate better with parameter β (involved in KAT equation and expressing HBA-basicity) than happens in case of the two rotaxanes **2a,b** (**Figure 8**).

For all three compounds the two main solvatochromic functional groups are the PCF and azo groups which both behave as fairly good HBA-bases being prone to formation of hydrogen bonds between the –CN and –N=N– groups respectively and

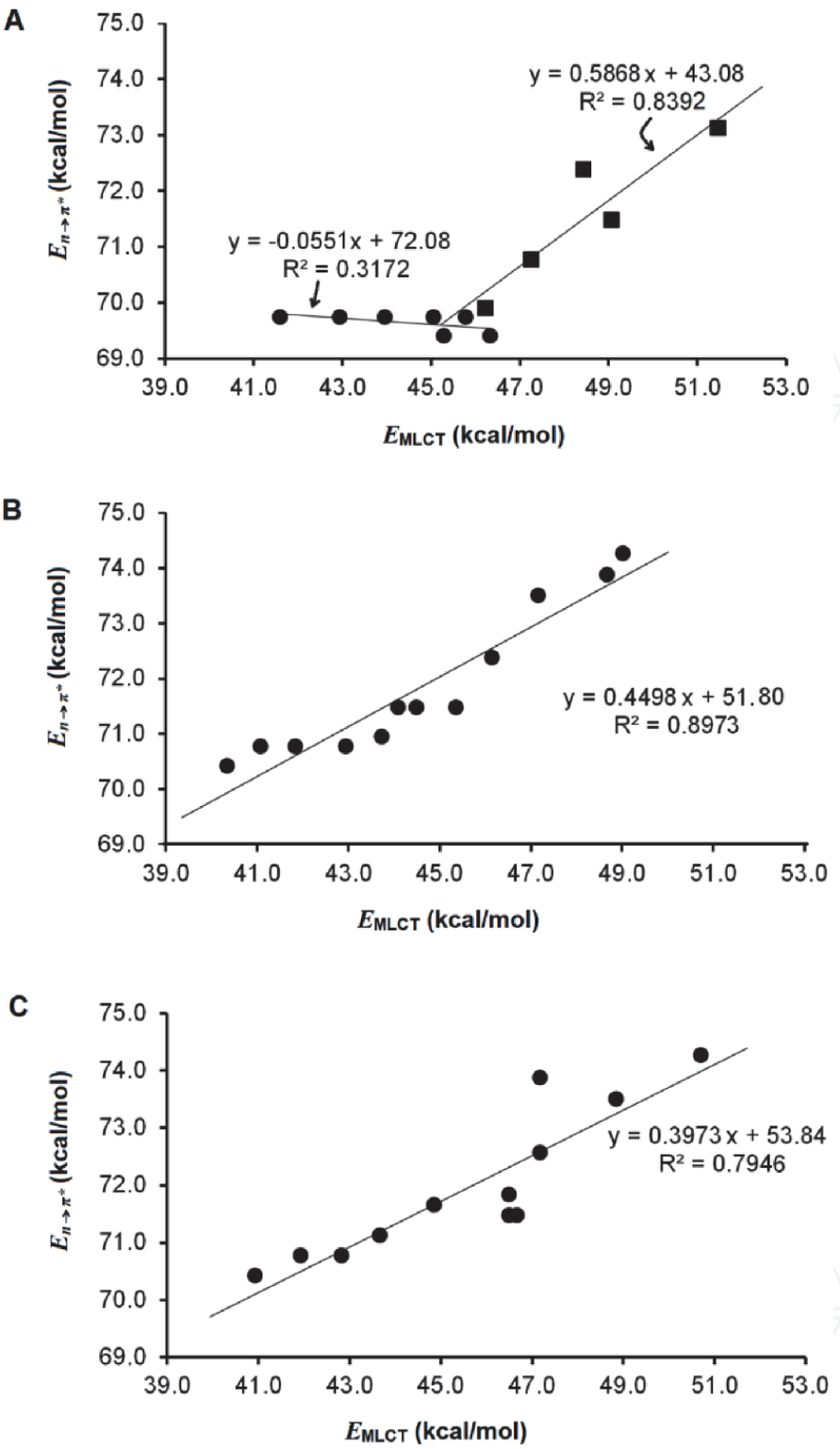

Figure 6.
Plots of the type $E_{n\to\pi^*}$ vsE_{MLCT} for (A) compound **1**, *(B) compound* **2a**, *and (C) compound* **2b**.

hydrogen atoms of protic solvents (like water and EG). Therefore, the nearly linear correlation observed between $E_{n\to\pi^*}$ and parameter β for compound **1**, indicates another type of solute-solvent interaction less pronounced in rotaxanes **2a,b** (**Figure 5**). The *ortho*-hydrogen atoms of pyridinium salts lying very close to the quaternized nitrogen are known to undergo deuterium-exchange [49–51]. The *ortho*-protons are significantly deshielded with chemical shifts around 9 ppm and sometimes close to 10 ppm (9.30 for **1**, 9.28 for **2b** and 9.27 ppm for **2a**) [19]. It is therefore anticipated that these hydrogen atoms are prone to interactions with polar

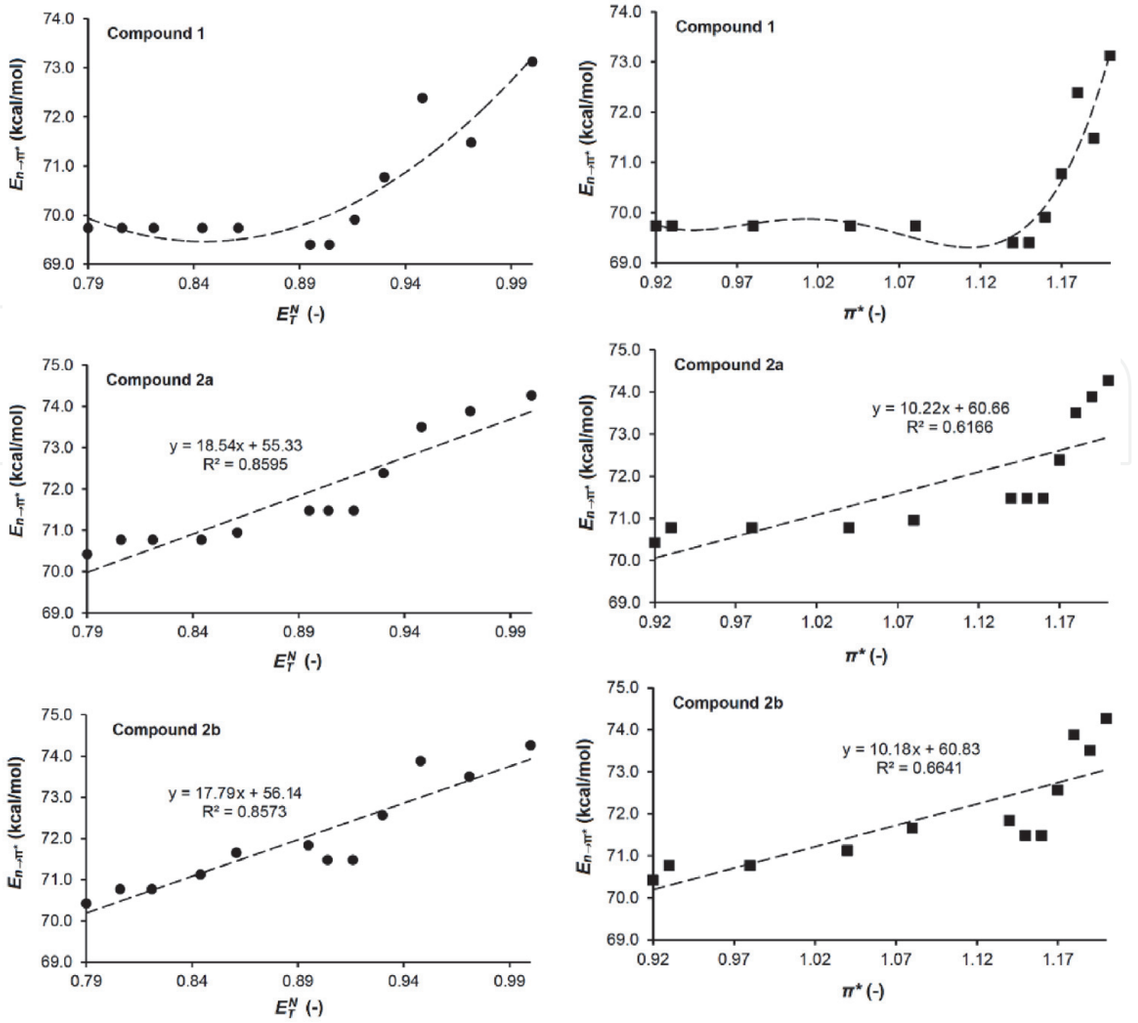

Figure 7.
Left column: *Plots of $n \rightarrow \pi^*$ energies determined in aqueous EG mixtures* vs *Reichardt's solvent polarity scale for compounds* **1**, **2a** *and* **2b**. *Right column: Plots of $n \rightarrow \pi^*$ energies determined in aqueous EG mixtures* vs *solvent polarity parameter π^* for compounds* **1**, **2a** *and* **2b** *[48].*

solvent molecules. Nevertheless, due to the presence of *alpha-* or *beta-* CyD in compounds **2a** and **2b** this interaction is somewhat hindered when compared to the CFD precursor **1**. In the latter case the *ortho*-hydrogen atoms can freely interact with the solvent molecules which in this particular case of interaction behave as HBA-bases. This interaction can clearly influence the $n \rightarrow \pi^*$ energy of **1**, as this region lies very close to the azobenzene group but also due to π-conjugation between the azobenzene group and the viologen.

Taken together, compound **1**, behaves differently than compounds **2a,b** and constitutes an interesting case where the two solvatochromic functional groups provide significantly different "information" about the polarity effects in their vicinity. In other words, based on SSP-LSERs compound **1** clearly behaves as a solvatochromic compound with dual sensitivity. The overall situation for all three compounds is schematically illustrated in **Figure 9** where the degree of success of each SSP-LSER is marked with colors (**Table 2**).

3.6 Multiprameteric LSERs

An alternative way to compare and quantify the solvatochromism of the two solvatochromic chromophores for **1** and **2a,b** is by employing the multiparametric LSERs. Such LSERs may involve various solvent polarity parameters, each of them

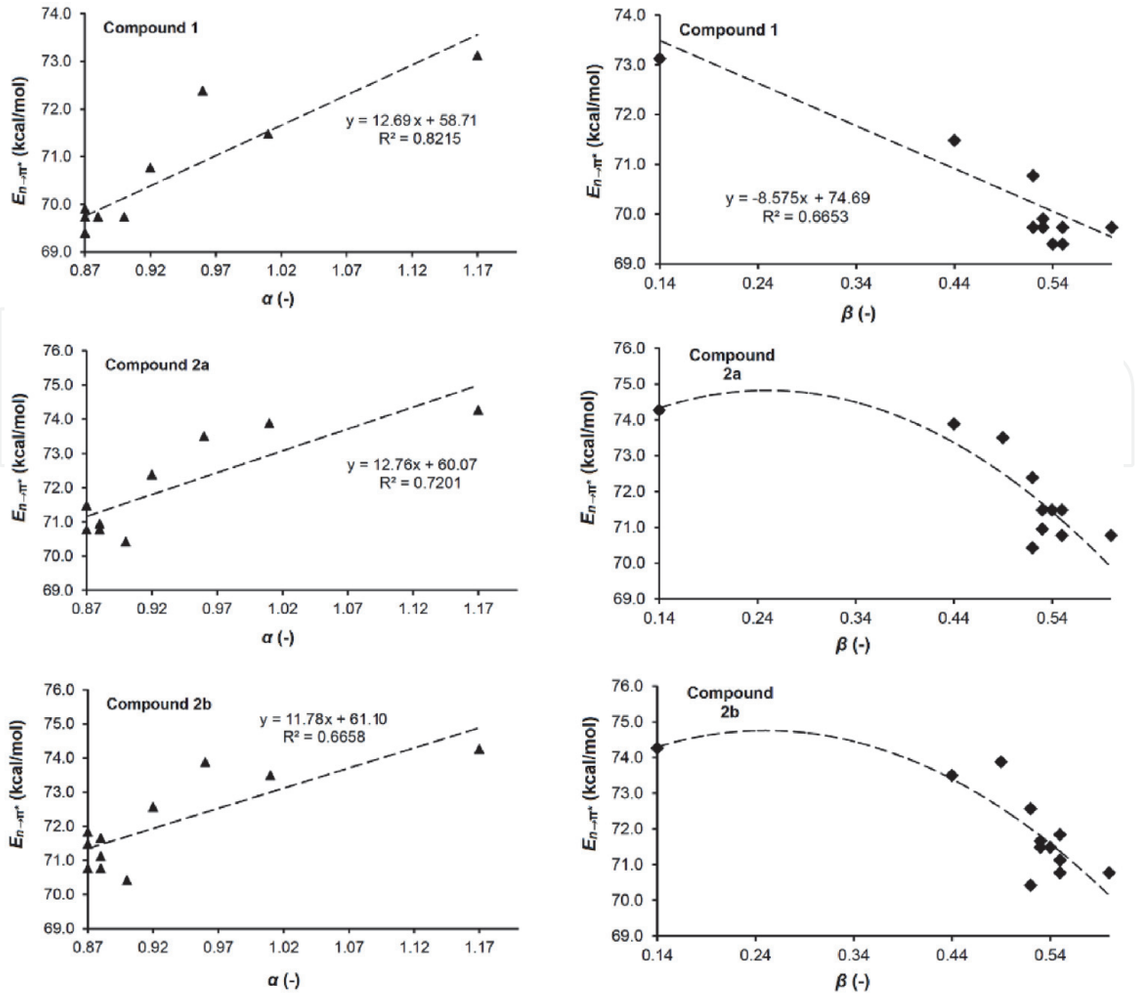

Figure 8.
Left column: Plots of n → π energies determined in aqueous EG mixtures* vs *solvent polarity parameter* α *for compounds* **1**, **2a** *and* **2b**. *Right column: Plots of n → π* energies determined in aqueous EG mixtures* vs *solvent polarity parameter* β *for compounds* **1**, **2a** *and* **2b** *[48].*

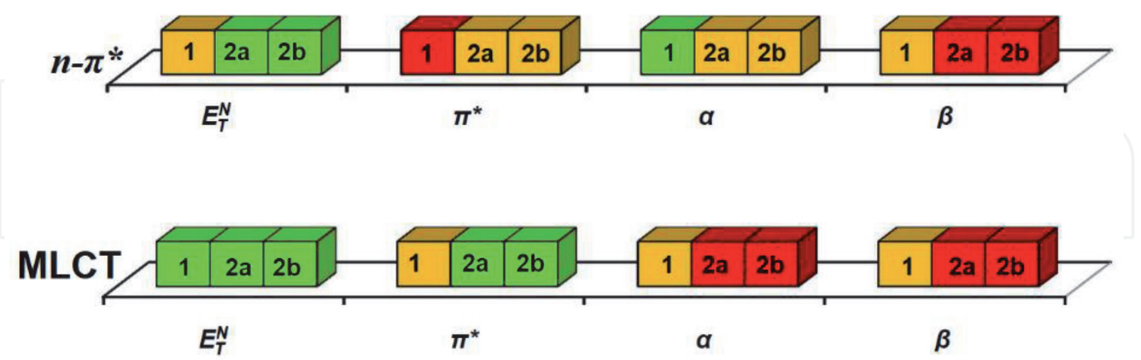

Figure 9.
Illustration depicting the goodness of linear fit between $E_{n\rightarrow\pi^*}$ *or* E_{MLCT} *and a SPP* (E_T^N, π*,α, *or* β). *Colors are based on correlation coefficients of the fits* (r^2). *Color code: Red:* $r^2 < 0.55$; *orange* $0.55 \leq r^2 \leq 0.79$; *green:* $r^2 > 0.79$.

describing a property of a solvent (or a solvent mixture). A prominent member of the family of such relationships is Kamlet-Abboud-Taft (KAT) equation which can provide information on the solvent polarity effect on various physicochemical properties in terms of specific and non-specific solute-solvent interactions [47]. Deligkiozi et al. employed the triparametric KAT equation (see Eq. 7) and found that for the solvatochromism of the PCF groups (MLCT transitions) in **1** and **2a,b**

	Dimesionless BSM polarity parameters[a]			
x_{EG}	$E_T^N(-)$	$\pi^*(-)$	$\alpha(-)$	$\beta(-)$
0	1.000	1.20	1.17	0.14
0.051	0.971	1.19	1.01	0.44
0.097	0.948	1.18	0.96	0.49
0.139	0.930	1.17	0.92	0.52
0.178	0.916	1.16	0.87	0.53
0.212	0.904	1.15	0.87	0.54
0.245	0.895	1.14	0.87	0.55
0.392	0.861	1.08	0.88	0.53
0.492	0.844	1.04	0.88	0.55
0.659	0.821	0.98	0.87	0.60
0.854	0.806	0.93	0.88	0.55
1	0.790	0.92	0.90	0.52

[a]*The values of the BSM polarity parameters are based on published data [52, 53] and they were determined through polynomial interpolation.*

Table 2.
Solvent polarity parameters employed in this work for the quantification of solvent plarity effects in aqueous EG mixtures.

Compound	E_0[†]	s[†]	a[†]	b[†]	$\%P_{\pi^*}$	$\%P_\alpha$	$\%P_\beta$	*rse*	r^2
	***n*(*azo*)→*π**(*azo*) Transitions**								
1	41.70	2.106	23.58	9.370	14.07	51.05	34.88	0.4687	0.8973
2a	36.73	6.425	24.15	11.64	34.70	39.18	26.12	0.2422	0.9762
2b	41.37	6.902	19.94	9.330	40.71	35.11	24.18	0.3461	0.9473
	***dp*(Fe^{II})→*π**(bpy) Transitions (MLCT)**								
1	5.724	17.50	20.44	4.753	51.27	26.63	22.10	0.6124	0.9630
2a	−11.10	20.42	28.96	13.26	58.56	23.77	17.67	0.3999	0.9854
2b	16.34	22.53	6.521	−2.764	64.66	18.21	17.13	0.4214	0.9845

[†]*Units: kcal/mol.*
rse*: residual standard error is the square root of the residual sum of squares divided by the residual degrees of freedom (here 8 for all cases).*

Table 3.
Results of the correlation of experimental **n→π*** *and MLCT energies of* ***1*** *and* ***2a-b*** *with KAT equation parameters.*

both specific and non-specific interactions are important at various extents depending on the compound (results are summarized in **Table 3**) [19]. Herein, the author reports the corresponding results pertaining to the solvatochromism of the azo group ($n \rightarrow \pi^*$ transitions). By use of Eqs. 8 and 9 (contribution analysis) the relative contribution of each of the parameters π*, α, and β was quantified (detailed results in **Table 3**). Through this analysis it can easily be made clear that for all three compounds the relative importance of the parameters π^*, α, and β, on the energy of the $n \rightarrow \pi^*$ is different when compared to the MLCT transitions. In case of MLCT transitions, parameter π^* appears to contribute the most for all three

compounds (%P_{π^*} ranging from 51.27 to 64.66%). Specific solute-solvent interactions described by HBA-basicity (parameter β) and HBD-acidity (parameter α) appear to demonstrate almost equal contribution. In other words, specific and non-specific interactions are almost evenly weighted when it comes to MLCT transitions and that is true for all three compounds. The situation gets way different when interpreting $n\rightarrow\pi^*$ transitions in the same fashion.

The behavior of compound **1** becomes different than those of compound **2a** and **2b,** and the uniformity of the contribution pattern that the MLCT transitions exhibit is lost. While for compound **1** HBD-acidity is the most contributing property (expressed through parameter α) compounds **2a** and **2b** exhibit almost equal contributions of all parameters π^*,α, and β. This is easily explained if the role of CyD (*alpha-* or *beta-*) is taken into account. As analyzed, in these [2]rotaxanes the CyD wheel preferably resides in the region of the azobenzene moiety so as to reduce the interaction with the ionic viologen parts of the axial molecule [54]. This effect hinders solvent molecules from interacting directly and specifically with the azo group (note that the azo group is highly prone to act as HBA-basic group; see **Figure 5B**). In case of **1** i.e. the CFD-precursor of these [2]rotaxanes, the lack of the CyD wheel renders the azo group-solvent interactions highly probable (**Figure 5B**). Therefore, **1** exhibits polarity responsive $n\rightarrow\pi^*$ transitions mainly influenced by parameter α. This constitutes a major differentiation among the studied compound and of course also between the two types of transitions. Obviously, the two transitions discussed herein convey spectrally different polarity information and that holds true for all three compounds but mostly for compound **1**.

3.7 PS effects as sensed by the FC and azo groups

It is well established that when a polar compound is dissolved in a BSM consisted of two solvents of different polarity, the compound/solute gets solvated selectively by one of the two solvents [17, 18]. This effect is obviously associated with preferential solute-solvent interactions developed in the vicinity of the solute molecules. Due to this effect the region around the solute (the so-called cybotactic region) is characterized by a different solvent/cosolvent molar ratio when compared to the bulk part of the solution i.e. the regions away from the cybotactic region. This interesting phenomenon, is attenuated when the two solvents consisting the BSM are similar in terms of structure and polarity [18]. There are numerous published models allowing for the quantification of selective solvation phenomena applicable to various types of solutes and BSMs. These models are generally categorized in thermodynamic and spectroscopy-based models [18]. In the latter case a solvatochromic solute is often employed in order to probe preferential solvation phenomena in BSMs and using spectrally measured shifts as inputs one can obtain various types of information pertaining to preferential solvation as output e.g. the solvent and cosolvent molar ratios in the cybotactic region. Through various spectroscopy-based models thermodynamic properties can also be determined for instance the molar free energy of transfer of the solute from one solvent to its cosolvent [18]. In this work preferential solvation of compounds **1** and **2a,b** in BSMs shall be used as a tool to rationalize the responsiveness of the two types of probing chromophores encompassed in these solvatochromic compounds i.e. the FC and azo groups.

By plotting the experimentally determined MLCT and $n\rightarrow\pi^*$ transition energies of **1** and **2a,b** at various water/EG mole fractions against the mole fraction of water or EG one can easily realize that for both types of transitions a significant deviation from linearity exists (see **Figure 10**). For all compounds the measured energies for either of the transitions MLCT or $n\rightarrow\pi^*$ were lower than the ideal/linear situations

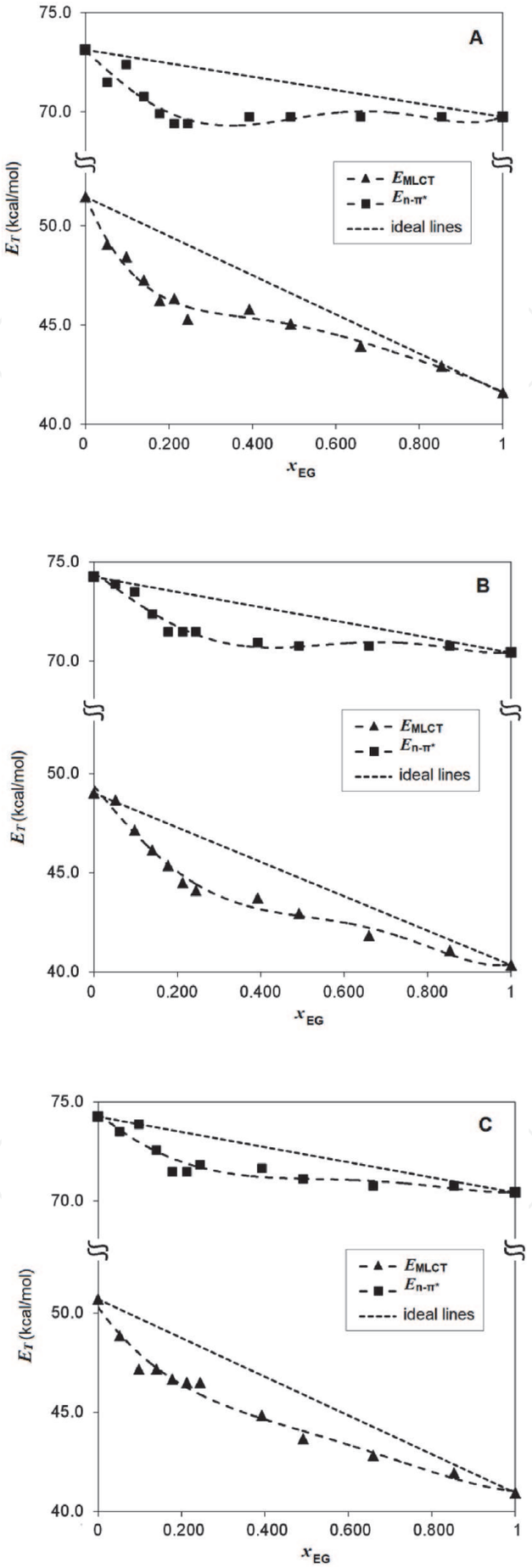

Figure 10.
Plots of experimental transition (MLCT or n→π) energies measured in aqueous EG, against the bulk mole fraction of EG for A) compound 1, B) [2] rotaxane* ***2a****, and C) [2]rotaxane* ***2b****.*

(dashed lines in **Figure 10**). Given the fact that both probing chromophores FC and azo, exhibit negative solvatochromism (i.e. increase of transition energy, or hypsochromism, when solvent polarity increases) the plots of **Figure 10** all describe preferential solvation of compounds **1**,**2a** and **2b** by EG (as will be thoroughly analyzed below). Indeed this effect has been thoroughly discussed in a recent paper by Papadakis et al. pertaining solely to the MLCT transitions. However, the new finding here is that the same effect is beautifully probed also by the azo group at least qualitatively. As can be easily seen, the shape of the non-linear $E_T = f(x_{EG})$ curves of **Figure 10** have very similar shapes for the both types of transitions. It is for instance apparent that the maximization of the linear deviation occurs in all six plots depicted at bulk molar ration of EG $0.15 \leq x_{EG} \leq 0.25$ i.e. in the water-rich bulk solvent composition region. Yet, important differences are revealed when the results are treated quantitatively through the TPMS model by Bagchi and coworkers [32] (details in the Materials and Methods section).

First of all, through the TPMS quantitative treatment the composition of the cybotactic region of solutions of **1** and **2a,b** were determined (see **Table 4**). Compound **1** appears to behave differently than the [2]rotaxanes (**2a,b**). The local EG mole fractions predicted by the same model for the MLCT and azo transition (y_{EG}^{mlct} and $y_{EG}^{n\rightarrow\pi^*}$ respectively) of **1** differ a lot. Interestingly, $y_{EG}^{n\rightarrow\pi^*}$ exhibits a propensity to maximize to the value of **1** (which denotes total solvation by EG) at a very low x_{EG} (x_{EG} = 0.212) whereas y_{EG}^{mlct} follows a much more "legitimate" increase and maximizes only in neat EG. For compounds **2a** and **2b**, y_{EG}^{mlct} and $y_{EG}^{n\rightarrow\pi^*}$ exhibit a very similar increase rate when going from neat water to neat EG (**Table 4**).

This becomes more obvious when plotting the δ_{EG} values obtained through the TPMS model against the bulk EG mole fractions (note: $\delta_{EG} = y_{EG} - x_{EG}$) as predicted through the experimentally observed MLCT and $n\rightarrow\pi^*$ energies. Apparently, compound **1** a different behavior compared to the [2]rotaxanes. The δ_{EG} predicted using the MLCT energies are significantly smaller than those predicted using $n\rightarrow\pi^*$ energies (**Figure 11A**). The difference in δ_{EG} drops when *alpha*-CyD is on (compound **2a**, **Figure 11B**) and drops even more when *beta*-CyD is threaded around the azobenzene group (compound **2b**, **Figure 11C**). In fact only δ_{EG} predicted using

x_{EG}	Compound 1		Compound 2a		Compound 2b	
	y_{EG}^{mlct}	$y_{EG}^{n\rightarrow\pi^*}$	y_{EG}^{mlct}	$y_{EG}^{n\rightarrow\pi^*}$	y_{EG}^{mlct}	$y_{EG}^{n\rightarrow\pi^*}$
0	0	0	0	0	0	0
0.051	0.569	0.660	0.510	0.526	0.553	0.555
0.097	0.590	0.561	0.560	0.555	0.610	0.526
0.139	0.635	0.766	0.599	0.662	0.610	0.642
0.178	0.681	0.952	0.634	0.784	0.630	0.784
0.212	0.675	1.000	0.676	0.784	0.637	0.784
0.245	0.728	1.000	0.698	0.784	0.637	0.731
0.392	0.702	1.000	0.719	0.880	0.714	0.757
0.492	0.740	1.000	0.770	0.917	0.782	0.846
0.659	0.807	1.000	0.853	0.917	0.838	0.917
0.854	0.880	1.000	0.922	0.917	0.907	0.917
1	1	1	1	1	1	1

Table 4.
Preferential solvation results obtained through the PS model.

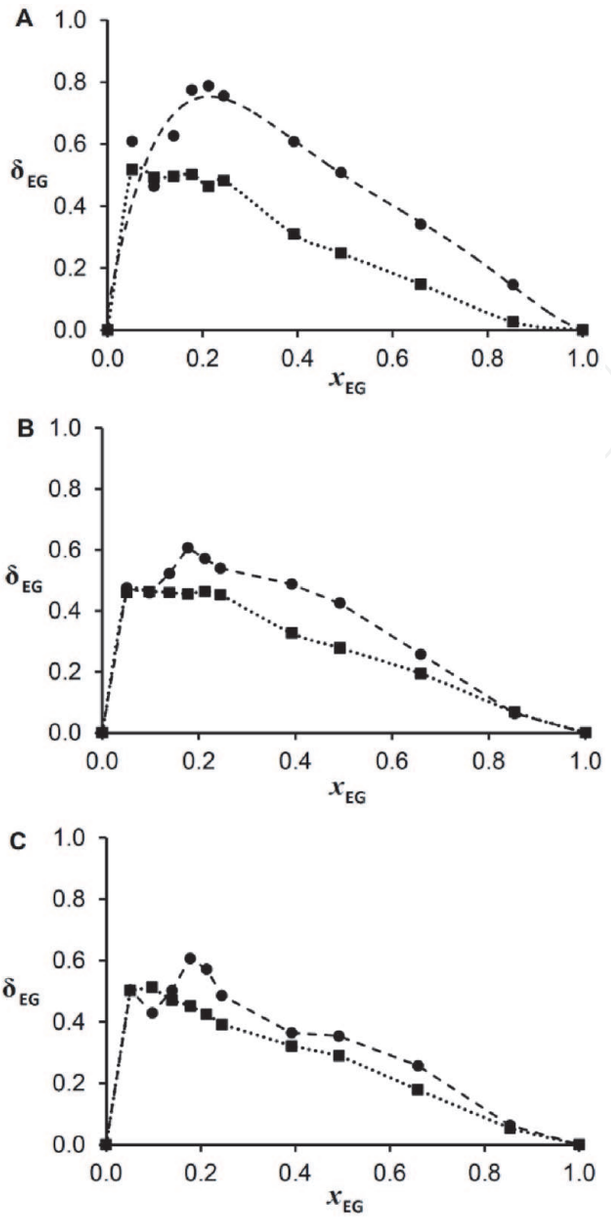

Figure 11.
*Plots of TPMS- predicted $\delta_{EG} = y_{EG} - x_{EG}$ versus the bulk EG mole fraction for A) **1**, B) **2a** and C) **2c**. Circles and dashed lines correspond to the prediction based on the azo-group whereas squares and dotted lines correspond to the prediction based on the FC group.*

	Compound 1	Compound 2a	Compound 2b
$x_{iso}^{mlct}(EG)$	0.18	0.20	0.30
$x_{iso}^{n\to\pi^*}(EG)$	0.055	0.15	0.13
$\Delta\int$	0.18	0.070	0.047
${}^{*}\Delta_{mlct}^{n\to\pi^*}(x_{iso})$	0.12	0.053	0.17

Table 5.
*Isosolvation points and $\Delta\int$ results for compounds **1** and **2a,b** in aqueous EG.*

$n\to\pi^*$ energies of compound **1** obtain values as high as 0.8. In other words, the azo group of compound **1** "feels" an excess of EG mole fraction of roughly 0.6 when the bulk EG mole fraction is only 0.2. Such large a preferential effect is not probed by the rest of the compounds. By integrating the differences in δ_{EG} for the three compounds one can easily see a decrease in $\Delta\int$ following the sequence:

$\Delta\int(\mathbf{1}) = 0.19 > \Delta\int(\mathbf{2a}) = 0.071 > \Delta\int(\mathbf{2b}) = 0.046$). Similar conclusions can be drawn when comparing the isosolvation points for the different probes of all compounds (**Table 5**). The results clearly illustrate a different probing aptitude of preferential solvation by the azo group of compound **1**. Of course all results indicate qualitatively the same PS effect i.e. EG is the preferred solvent in the cybotactic region at all measured mole fractions.

4. Conclusions

A general conclusion of the present study is that two distinct functional groups acting as chromophores (specifically the FC and azo groups) can probe solvation effects in different ways however this is true only on a quantitative basis. Qualitatively, both functional groups probed a strong negative solvatochromic effect in all cases of molecules studied. It became apparent though that FC is more sensitive to the dipolarity/polarizability of the medium whereas the azo group is slightly more responsive to polarity changes associated to the Lewis acidity and HBD-acidity of the medium. This holds true for compound **1** and **2a** but not for compound **2b** where the bulkiness of *beta*-CyD hinders any azobenzene-solvent direct interaction. In that case (**2b**) the azo group appears to have very similar sensitivity to solvent polarity to that that the FC group exhibits. On the other hand, both functional groups probed an intense PS effect by EG molecules however for each compound different extents in PS were probed. Compound **1**, again appeared to behave differently on a quantitative basis. The difference in probed extent PS between the azo and the FC group was the largest for **1** and dropped significantly in case of the *alpha*- or *beta*-CyD comprising [2]rotaxanes (compounds **2a**, and **2b**). Overall, compound **1**, exhibits a distinct dual sensing aptitude in terms of solute-solvent specific and non-specific effects as well as PS effects. The [2]rotaxanes have a rather attenuated dual sensing capacity presumably due to the presence of CyD which hinders the direct interaction of the azo-group (and its surrounding regions) with solvent molecules. As a result of the extended π-conjugation and the "shielding" effect of CyD the azo groups of compounds **2a** and **2b** tend to probe the same solvent polarity information as the FC group. It is important to mention that compound **1** clearly exhibits a dual solvatochromic behavior, however in water/EG BSMs the response of the azo group gets saturated to the value corresponding to neat EG very fast as one moves from neat water to neat EG (see **Table 4**). Nonetheless, as analyzed this corresponds to a special PS effect and taken together compound **1**, appears to be a very good polarity sensor candidate for future application mainly pertaining to polar media such as water solutions and mixtures with polar organic solvents.

Acknowledgements

The author would like to thank Dr. D. Matiadis (NCSR Demokritos, Athens, Greece) for fruitful discussions revolving around the solvatochromism of heterocyclic compounds. IKY (Greek State Scholarship Foundation) is gratefully acknowledged for financial support to R.P. during his PhD; a part of this work is connected to the work carried out then.

Notes

The authors declare no competing financial interest.

Author details

Ioanna Deligkiozi[1] and Raffaello Papadakis[1,2*]

1 Laboratory of Organic Chemistry, School of Chemical Engineering, National Technical University of Athens (NTUA), Athens, Greece

2 TdB Labs, Uppsala, Sweden

*Address all correspondence to: rafpapadakis@gmail.com

IntechOpen

References

[1] Liu, H.; Xu, X.; Peng, H.; Chang, X.; Fu, X.; Li, Q.; Yin, S.; Blanchard G. J.; Fang, Y. New solvatochromic probes: Performance enhancement via regulation of excited state structures. **Phys. Chem. Chem. Phys.**, **2016**,*18*, 25210-25220. DOI: 10.1039/C6CP04293G.

[2] Ali, R.; Lang, T.; Saleh, S. M.; Meier, R. J. Wolfbeis O. S. Optical sensing scheme for carbon dioxide using a Solvatochromic probe. Anal. Chem., **2011**, *83*, 2846-2851. DOI: 10.1021/ac200298j.

[3] Landis, R. F.; Yazdani, M.; Creran, B.; Yu, X.; Nandwana, V.; Cooke, G.; Rotello. V. M. Solvatochromic probes for detecting hydrogen-bond-donating solvents. *Chem. Commun.*, **2014**, *50*, 4579-4581. DOI: 10.1039/C4CC00805G.

[4] Florindo, C.; McIntosh, A. J. S.; Welton, T. ; Brancod, L. C.; Marrucho. I. M. A closer look into deep eutectic solvents: exploring intermolecular interactions using solvatochromic probes. *Phys. Chem. Chem. Phys.*, **2018**, *20*, 206-213. DOI: 10.1039/C7CP06471C.

[5] Liu, H,; Xu, X.; Shi, Z.; Liu, K.; Yu, L.; Fang Y. Solvatochromic probes displaying unprecedented organic liquids discriminating characteristics. Anal. Chem., **2016**, *88*, 10167-10175. DOI: 10.1021/acs.analchem.6b02721.

[6] Li, Z.; Askim, J. R.; Suslick, K. S. The optoelectronic nose: Colorimetric and Fluorometric sensor arrays. Chem. Rev. **2019**, *119*, 231-292. DOI: 10.1021/acs.chemrev.8b00226.

[7] Machado, V. G.; Stock, R. I.; Reichardt, C. Pyridinium N-Phenolate Betaine Dyes. *Chem. Rev.* **2014**, *114*, 10429-10475. DOI: 10.1021/cr5001157.

[8] Reichardt, C. Solvatochromic dyes as solvent polarity indicators. Chem. Rev.**1994**, *94*, 2319-2358. DOI: 10.1021/cr00032a005.

[9] Cabota, R.; Hunter, C. A. Molecular probes of solvation phenomena. Chem. Soc. Rev., **2012**, *41*, 3485-3492. DOI: 10.1039/C2CS15287H.

[10] Reichardt, C.; Welton. T. Solvents and solvent effects in organic chemistry. 4th Edn. Wiley-VCH, 2011, Weinheim.

[11] Eilmes, A. Kubisiak, P. Explicit solvent modeling of Solvatochromic probes in ionic liquids: Implications of solvation Shell structure. J. Phys. Chem. B, **2015**, *119*, 113185-113197. DOI: 10.1021/acs.jpcb.5b07767.

[12] Khajehpour, M.; Welch, C. M. Kleiner, K. A. Kauffman J. F. Separation of dielectric nonideality from preferential solvation in binary solvent systems: An experimental examination of the relationship between Solvatochromism and local solvent composition around a dipolar solute. J. Phys. Chem. A, **2001**, *105*, 5372-5379. DOI: 10.1021/jp010825a.

[13] Duereh, A.; Sato, Y.; Smith, R. L.; Inomata, H. Spectroscopic analysis of binary mixed-solvent-polyimide precursor systems with the preferential solvation model for determining solute-centric Kamlet–Taft Solvatochromic parameters. J. Phys. Chem. B, **2015**, *119*, 14738-14749. DOI: 10.1021/acs.jpcb.5b07751.

[14] Papadakis, R. Preferential solvation of a highly medium responsive Pentacyanoferrate(II) complex in binary solvent mixtures: Understanding the role of dielectric enrichment and the specificity of solute−solvent interactions. J. Phys. Chem. B, **2016**, *120*, 9422-9433. DOI: 10.1021/acs.jpcb.6b05868

[15] Papadakis, R. Solute-centric versus indicator-centric solvent polarity

parameters in binary solvent mixtures. Determining the contribution of local solvent basicity to the solvatochromism of a pentacyanoferrate(II) dye. J. Mol. Liq. **2017**, *241*, 211–221. DOI: 10.1016/j.molliq.2017.05.147

[16] Papadakis, R. The solvatochromic behavior and degree of ionicity of a synthesized pentacyano (N-substituted-4,40-bipyridinium) ferrate(II) complex in different media. Tuning the solvatochromic intensity in aqueous glucose solutions. Chem. Phys., **2014**, *430*, 29-39. DOI: 10.1016/j.chemphys.2013.12.008.

[17] Ben-Naim, A. Theory of preferential solvation of nonelectrolytes. Cell Biophys. **1988**, *12*, 255-269. DOI: 10.1007/BF02918361.

[18] Marcus, Y. Solvent mixtures: Properties and selective solvation, Marcel Dekker, Inc., 2002, New York.

[19] Deligkiozi, I; Voyiatzis, E.; Tsolomitis, A.; Papadakis, R. Synthesis and characterization of new azobenzene-containing bis pentacyanoferrate(II) stoppered push–pull [2]rotaxanes, with α- and β-cyclodextrin. Towards highly medium responsive dyes. Dyes Pigment., **2015**, *113,* 709-722. DOI: 10.1016/j.dyepig.2014.10.005.

[20] Qu, D-H.; Ji, F-Y.; Wang, Q-C.; Tian H. A double INHIBIT logic gate employing configuration and fluorescence changes. Adv. Mater. **2006**, *18*, 2035-2038. DOI: 10.1002/adma.200600235.

[21] Baroncini, M.; Gao, C.; Carboni, V.; Credi, A.; Previtera, E.; Semeraro, M.; Venturi, M.; Silvi, S. Light control of stoichiometry and motion in pseudorotaxanes comprising a cucurbit[7]uril wheel and an azobenzene-bipyridinium axle. Chem. Eur. J. **2014**, *20*, 10737-10744. DOI: 10.1002/chem.201402821.

[22] Qu, D-H.; Wang, Q-C.; Tian, H. A half adder based on a photochemically driven [2] rotaxane. Angew. Chem. Int. Ed., **2005**, *44*, 5296-5299. DOI: 10.1002/anie.200501215.

[23] Monk, P.M.S. The viologens: Physicochemical properties, synthesis and applications of the salts of 4,40-Bipyridine. John Wiley & Sons ltd; 1998, Chichester.

[24] Crano, J.C.; Guglielmetti, R.J. (Eds). Organic photochromic and thermochromic compounds. Main photochromic families, vol. 1. Kluwer Academic Publishers; 2002. New York. p. 341-67.

[25] Deligkiozi, I.; Tsolomitis, A.; Papadakis, R. Photoconductive properties of a π-conjugated α-cyclodextrin containing [2]rotaxane and its corresponding molecular dumbbell. Phys. Chem. Chem. Phys., **2013**,*15*, 3497-3503. DOI: 10.1039/C3CP43794A

[26] Papadakis, R.; Deligkiozi, I.; Giorgi, M.; Faure, B.; Tsolomitis, A. Supramolecular complexes involving non-symmetric viologen cations and hexacyanoferrate (II) anions. A spectroscopic, crystallographic and computational study. RSC Adv., **2016**, *6*, 575-585. DOI: 10.1039/C5RA16732A.

[27] Papadakis, R; Deligkiozi, I; Tsolomitis A. Synthesis and characterization of a group of new medium responsive non-symmetric viologens. Chromotropism and structural effects. Dyes Pigment., **2012**, *95*, 478-484. DOI: 10.1016/j.dyepig.2012.06.013.

[28] Papadakis, R; Deligkiozi, I; Tsolomitis A. Spectroscopic investigation of the solvatochromic behavior of a new synthesized non symmetric viologen dye: Study of the solvent-solute interactions. Anal. Bioanal. Chem. **2010**, *397*, 2253-2259. DOI: 10.1007/s00216-010-3792-7.

[29] Zhu, Y; Zhou, Y; Wang, X. Photoresponsive behavior of two well-defined azo polymers with different electron-withdrawing groups on pushepull azo chromophores. Dyes Pigment., **2013**, *99*, 209-219. DOI: 10.1016/j.dyepig.2013.05.006.

[30] Papadakis, R.; Tsolomitis, A. Study of the correlations of the MLCT Vis absorption maxima of 4-pentacyanoferrate- 4-arylsubstituted bispyridinium complexes with the Hammett substituent parameters and the solvent polarity parameters ETN and AN. J. Phys. Org. Chem. **2009**, *22*, 515-521. DOI: 10.1002/poc.1514.

[31] Papadakis, R.; Tsolomitis, A. Solvatochromism and preferential solvation of 4-pentacyanoferrate 4-aryl substituted bipyridinium complexes in binary mixtures of hydroxylic and non-hydroxylic solvents. J. Solut. Chem., **2011**, *40*, 1108-1125. DOI: 10.1007/s10953-011-9697-z.

[32] Chatterjee, P.; Bagchi, S. Preferential solvation of a dipolar solute in mixed binary solvent: A study of UV-visible spectroscopy. J. Phys. Chem. **1991**, *95*, 3311-3314. DOI: 10.1021/j100161a064.

[33] Banerjee, D.; Laha, A.K.; Bagchi, S. Preferential solvation in mixed binary solvent. J. Chem. Soc. Faraday Trans., **1995**, *91*, 631-636. DOI: 10.1039/FT9959100631.

[34] Laha, A.K.; Das, P.K.; Bagchi, S. Study of preferential solvation in mixed binary solvent as a function of solvent composition and temperature by UV-vis spectroscopic method. J. Phys. Chem. A, **2002**, *106*, 3230-3234. DOI: 10.1021/jp0121116.

[35] Redlich, O.; Kister, A.T.. Algebraic representation of thermodynamic properties and the classification of solutions. Ind. Eng. Chem.**1948**, *40*, 345-348. DOI: 10.1021/ie50458a036.

[36] Krygowski, T.M.; Fawcett, W. R. Complementary Lewis acid-base description of solvent effects. I. Ion-ion and ion-dipole interactions. *J. Am. Chem. Soc.*, **1975**, *97*, 2143-2148. DOI: 10.1021/ja00841a026.

[37] Papadakis, R.; Deligkiozi, I.; Nowak, E. K. Study of the preferential solvation effects in binary solvent mixtures with the use of intensely solvatochromic azobenzene involving [2] rotaxane solutes. J. Mol. Liq., **2019**, *274*, 715-723. DOI: 10.1016/j.molliq.2018.10.164.

[38] Hofmann, K.; Brumm, S.; Mende, C.; Nagel, K.; Seifert, A.; Roth, I.; Schaarschmidt, D.; Lang, H.; Spange, S. Solvatochromism and acidochromism of azobenzene-functionalized poly(vinyl amines). New J. Chem., **2012**, *36*, 1655–1664. DOI: 10.1039/c2nj40313g.

[39] Sıdır, Y. G.; Sıdır, I; Taşal¸ E., E. Ermiş. Studies on the electronic absorption spectra of some monoazo derivatives. *Spectrochim.* Acta A **2011,** *78*, 640–647. DOI: 10.1016/j.saa.2010.11.0.

[40] Gasbarri, C.; Angelini, G. Polarizability over dipolarity for the spectroscopic behavior of azobenzenes in room-temperature ionic liquids and organic solvents. J. Mol. Liq., **2017**, *229*, 185–188. DOI: 10.1016/j.molliq.2016.12.033.

[41] Qian, H-F.; Tao, T.; Feng, Y-N.; Wang, Y-G.; Huang, W. Crystal structures, solvatochromisms and DFT computations of three disperse azo dyes having the same azobenzene skeleton. J. Mol. Struct. **2016**, *1123*, 305-310. DOI: 10.1016/j.molstruc.2016.06.04.

[42] Christoforou, D. Electronic effects of the azo group. PhD Thesis, University of Canterbury, New Zealand, 1981.

[43] Mulski, M. J.; Connors, K.A. Solvent effects on chemical processes. 9. Energetic contributions to the

complexation of 4-nitroaniline with α-cyclodextrin in water and in binary aqueous-organic solvents. **1995**, *4*, 271-278. DOI: 10.1080/10610279508028936.

[44] Hickey, J.P.; Passlno-Reader D.R. Linear solvation energy relationships: "Rules of thumb" for estimation of variable values. Environ. Sci. Technol., **1991,** *25*, 1753-1760. DOI: 10.1021/es00022a012.

[45] Endo, S; Goss, K-U. Applications of Polyparameter linear free energy relationships in environmental chemistry. Environ. Sci. Technol., **2014**, *48*, 12477−12491. DOI: 10.1021/es503369t.

[46] Williams, A. Free Energy Relationships in Organic and Bio-Organic Chemistry. Royal Society of Chemistry, Cambridge UK, 2003.

[47] Kamlet, M.J.; Abboud, J.L.M.; Abraham, M.H.; Taft, R.W. Linear solvation energy relationships. 23. A comprehensive collection of the solvatochromic parameters, .Pi.*, . Alpha., and.Beta., and some methods for simplifying the generalized solvatochromic equation, *J. Organomet. Chem.* **1983**, *48,* 2877–2887. DOI: doi.org/10.1021/jo00165a018.

[48] The non-linear fit(s) in this figure correspond to polynomial fitting(s) and convey no physical meaning. They are simply used in order to visualize the sizable deviations from linearity.

[49] Ratts, K. W.; Howe, R. K.; Phillips, W. G. Formation of pyridinium ylides and condensation with aldehydes. J. Amer. Chem.Soc.**1969**, *91*, 6115-6121. DOI: 10.1021/ja01050a032.

[50] Zoltewicz, J. A.; Smith, C. L.; Kauffman, G. M. Buffer catalysis and hydrogen-deuterium exchange of heteroaromatic carbon acids. Heterocycl. Chem. **1971**, *8*, 337-338. DOI: 10.1002/jhet.5570080236.

[51] Elvidge, J.A.; Jones, J.R.; O'Brien, C.; Evans, E.A.; Sheppard, H.C. Base-Catalyzed Hydrogen Exchange. *Adv. Heterocycl. Chem.* **1974**, *16*, 1-31. DOI: 10.1016/S0065-2725(08)60458-4.

[52] Marcus, Y. The use of chemical probes for the characterization of solvent mixtures. Part 2. Aqueous mixtures. *J. Chem. Soc.* Perkin Trans. **1994**, *2*, 1751−1758. DOI: 10.1039/P2994000175

[53] Sindreu, R. J.; Moyá, M. L.; Sánchez Burgos, F.; González, A. G. Kamlet-Taft solvatochromic parameters of aqueous binary mixtures oftert-butyl alcohol and ethyleneglycol. J. Solut. Chem. **1996**, *25*, 289-293. DOI: 10.1007/BF00972526.

[54] Deligkiozi, I.; Papadakis, R.; Tsolomitis, A. Synthesis, characterisation and photoswitchability of a new [2]rotaxane of α-cyclodextrin with a diazobenzene containing π-conjugated molecular dumbbell. Supramol. Chem. **2012**, *24*, 333-343. DOI: 10.1080/10610278.2012.660529.